Effect of Coupling Point Selection on Distortion in Internet-distributed Hardware-in-the-Loop Simulation

Tulga Ersal, R. Brent Gillespie, Mark Brudnak, Jeffrey L. Stein, and Hosam K. Fathy

***Abstract*—Internet-distributed hardware-in-the-loop (ID-HIL) simulation integrates geographically-dispersed HIL setups and fosters concurrent systems testing early in the design process. The degree to which an ID-HIL simulation loses fidelity relative to the single-location alternative is referred to as *distortion*. The literature showed that various factors affect distortion, e.g., delay, jitter, and loss. This paper shows that the coupling points, i.e., the particular points at which the system model is divided to enable distribution across the Internet, also affect distortion. The aim is to turn coupling point selection into a design decision that can be used to minimize distortion. To quantify distortion, a frequency-domain metric is proposed using a linear systems framework. This metric is then used to analyze how the choice of the coupling point affects distortion, leading to guidelines for selecting a coupling point that gives minimal distortion. The theory is demonstrated on a quarter-car model.**

***Keywords*—coupling points; Internet-distributed hardware-in-the-loop simulation; delay systems; distortion**

I. INTRODUCTION

HARDWARE-IN-THE-LOOP simulation (HILS) refers to simulating a system by coupling the physical models of some of its components together with the mathematical models of its remaining components (Bacic et al. 2009). Thus, it combines the high fidelity of physical prototyping with the cost effectiveness of model-based simulation (Fathy et al. 2006). It strongly promotes concurrent system engineering and has therefore become indispensable in many application areas, such as automotive (Kimura and Maeda 1996; Zhang and Alleyne 2005; Verma et al. 2008), aerospace (Leitner 2001; Yue et al. 2005; Cai et al. 2009), manufacturing (Ganguli et al. 2005), robotics (Aghili and Piedboeuf 2002; White et al. 2009), and defense (Huber Jr and Courtney 1997; Buford et al. 2000).

To fully exploit the benefits of HILS, it may be desirable to integrate multiple HILS setups (Kelf 2001). Recent efforts have focused on achieving such integration over the Internet to allow for integration of setups that are geographically dispersed and unfeasible to couple physically. For example, the George E. Brown Jr. Network for Earthquake Engineering Simulation (NEES) (Mahin et al. 2003) provides an outstanding example of the capabilities and impact of the ID-HILS idea, and the earthquake literature presents many other applications of the ID-HILS idea to earthquake simulation (Watanabe et al. 2001; Tsai et al. 2003; Spencer et al. 2004; Pan et al. 2005; Stojadinovic et al. 2006; Mosqueda et al. 2008). Another example in the automotive application area is the integration of a ride motion simulator in Warren, MI, USA, with a hybrid-powertrain-system simulator in Santa Clara, CA, USA (Compere et al. 2006; Goodell et al. 2006; Brudnak et al. 2007) and, as a separate work, with an engine-in-the-loop simulator in Ann Arbor, MI, USA (Ersal et al. in press a; Ersal et al. in press b). These works highlight the potential impact of ID-HILS for automotive systems.

Coupling HILS setups over the Internet introduces a deviation from the dynamics that would otherwise be observed if the setups were collocated and could be directly integrated. This deviation is termed *distortion* in this paper.

There are several sources of distortion in an ID-HIL setup. Distributing a system into subsystems that are co-simulated using independent numerical solvers can be in and of itself an important source of distortion due to the lack of access to the Jacobians of the remote sites, sampling effects, etc., even without any delay (Ersal et al. in press b). Distribution over the Internet introduces further distortion due to the Internet's delay, jitter, and loss. Jitter refers to the variability of delay, and loss means that not all packets sent arrive at destination. Recognizing these issues, the literature proposed methods to assess the relative impact of distribution effects in comparison to the effects of the Internet's delay, jitter, and loss (Ersal et al. in press b). The literature also developed various approaches, e.g., passivity-based (Anderson and Spong 1989; Niemeyer and Slotine 1991; Niemeyer and Slotine 2002; Lee and Spong 2006), event-based (Xi and Tarn 2000; Elhajj et al. 2003; Mosqueda et al. 2008), and observer-based (Compere et al. 2006; Goodell et al. 2006; Brudnak et al. 2007) frameworks, to address stability and distortion issues under a delayed coupling of subsystems.

This paper focuses on another potential variable that can affect distortion, namely, the coupling point. Within the context of this paper, coupling point refers to the point at which the HILS system is divided into two subsystems that are then co-simulated. While options for placement of the coupling point may not always exist, when they do exit, the location of the coupling point can become a design parameter. Then, it becomes important to know how to best pick that design parameter to minimize distortion.

Thus, the aim of this paper is to develop a framework in which the impact of coupling point selection on distortion can be studied and the reasons that make one coupling point better than another can be understood. As a first step, this paper will consider only the delay and ignore the jitter, loss, and the distributed simulation effects (numerical issues due to separate solvers, sampling effects, etc.). This will not only simplify the problem, but also allow for the analysis to be handled through a linear framework. A linear framework will, in turn, allow for leveraging the existing frequency-domain

Report Documentation Page

Form Approved
OMB No. 0704-0188

1. REPORT DATE	2. REPORT TYPE	3. DATES COVERED
01 APR 2011	**N/A**	**-**

4. TITLE AND SUBTITLE	5a. CONTRACT NUMBER
Effect of Coupling Point Selection on Distortion in Internetdistributed Hardware-in-the-Loop Simulation (PREPRINT)	5b. GRANT NUMBER
	5c. PROGRAM ELEMENT NUMBER
6. AUTHOR(S)	5d. PROJECT NUMBER
Tulga Ersal; R. Brent Gillespie; Mark Brudnak; Jeffrey L. Stein; Hosam K. Fathy	5e. TASK NUMBER
	5f. WORK UNIT NUMBER
7. PERFORMING ORGANIZATION NAME(S) AND ADDRESS(ES)	8. PERFORMING ORGANIZATION REPORT NUMBER
US Army RDECOM-TARDEC 6501 E 11 Mile Rd Warren, MI 48397-5000, USA	**21554**
9. SPONSORING/MONITORING AGENCY NAME(S) AND ADDRESS(ES)	10. SPONSOR/MONITOR'S ACRONYM(S)
US Army RDECOM-TARDEC 6501 E 11 Mile Rd Warren, MI 48397-5000, USA	**TACOM/TARDEC/RDECOM**
	11. SPONSOR/MONITOR'S REPORT NUMBER(S) **21554**

12. DISTRIBUTION/AVAILABILITY STATEMENT
Approved for public release, distribution unlimited

13. SUPPLEMENTARY NOTES
Submitted for publication in a Special Issue of Int'l Journal of Vehicle Design, The original document contains color images.

14. ABSTRACT
AbstractInternet-distributed hardware-in-the-loop (IDHIL) simulation integrates geographically-dispersed HIL setups and fosters concurrent systems testing early in the design process. The degree to which an ID-HIL simulation loses fidelity relative to the single-location alternative is referred to as distortion. The literature showed that various factors affect distortion, e.g., delay, jitter, and loss. This paper shows that the coupling points, i.e., the particular points at which the system model is divided to enable distribution across the Internet, also affect distortion. The aim is to turn coupling point selection into a design decision that can be used to minimize distortion. To quantify distortion, a frequency-domain metric is proposed using a linear systems framework. This metric is then used to analyze how the choice of the coupling point affects distortion, leading to guidelines for selecting a coupling point that gives minimal distortion. The theory is demonstrated on a quarter-car model.

15. SUBJECT TERMS
coupling points; Internet-distributed hardware-in-the-loop simulation; delay systems; distortion

16. SECURITY CLASSIFICATION OF:			17. LIMITATION OF ABSTRACT	18. NUMBER OF PAGES	19a. NAME OF RESPONSIBLE PERSON
a. REPORT	b. ABSTRACT	c. THIS PAGE			
unclassified	**unclassified**	**unclassified**	**SAR**	**7**	

characterizations of distortion (Lawrence 1993; Yokokohji and Yoshikawa 1994; Çavuşoğlu et al. 2002; De Gersem et al. 2005; Griffiths et al. 2008).

The rest of the paper is organized as follows. A motivating example is given first in Section II that illustrates how the location of the coupling point can affect distortion in a quarter-car representation of a vehicle. Then, in Section III.A, a frequency-domain distortion metric from the haptics literature is adopted into the ID-HIL framework. Using this metric, Section III.B investigates which coupling point characteristics lead to a low distortion, and relates distortion to a sensitivity function. Section III.C establishes the signal-dependence of distortion, and Section III.D discusses the effect of causality on distortion. Finally, in Section IV, the theory developed is applied to the illustrative quarter-car example, and conclusions are drawn in Section V.

II. Motivating Example

Consider the system shown in Fig. 1, which is a quarter-car representation of a vehicle, where the masses m_1, m_2, and m_3 represent the unsprung, sprung, and driver masses, respectively, and the corresponding spring-damper pairs capture the tire, suspension, and seat stiffness and damping properties. The figure also shows the two coupling point candidates considered in this study, labeled as CP1 and CP2. The coupling variables at these coupling points and their causality are explicitly shown in Fig. 2. A constant time delay of τ is considered in both directions of communication, leading to a round-trip time delay of 2τ. The input is the road velocity input, and the output of interest is the displacement of the suspension. The parameter values of the system are given in Table I and are representative of a military vehicle (Ersal et al. 2009).

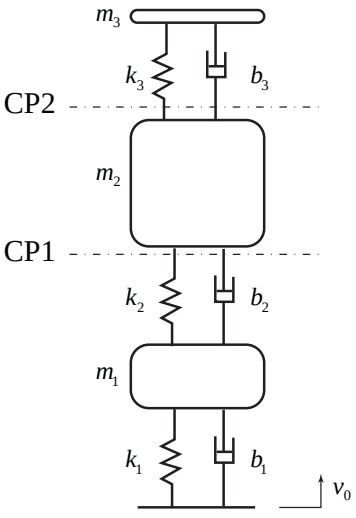

Fig. 1.Example system with two locations as potential coupling points

TABLE I
PARAMETERS OF THE EXAMPLE SYSTEM

Parameter	Value
b_1	200 kNs/m
b_2	30 kNs/m
b_3	250 Ns/m
k_1	1 MN/m
k_2	275 kN/m
k_3	1.4 kN/m
m_1	110 kg
m_2	900 kg
m_3	20 kg
τ	20 ms

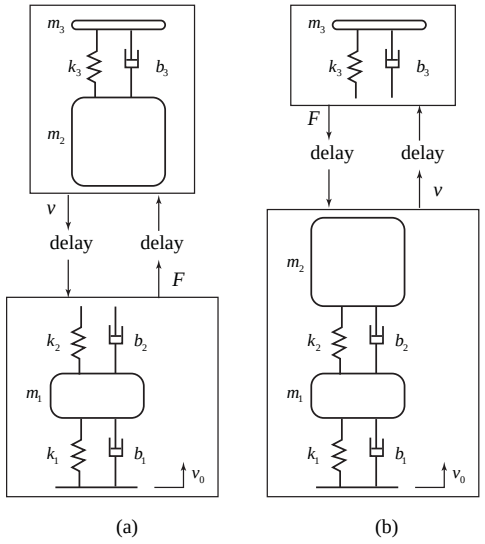

Fig. 2. Subsystems and coupling causality shown explicitly for (a) CP1 and (b) CP2

Fig. 3 compares the unit step responses of the ideal system and the two systems in which the coupling variables at CP1 and CP2 are communicated with the constant time delay of τ. As seen in the figure, a delay at CP1 causes much more distortion than a delay at CP2. This exemplifies the impact of the location of the coupling point on distortion and motivates the rest of the paper.

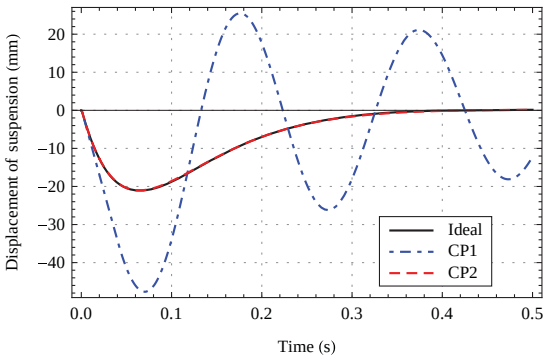

Fig. 3.Comparing the unit step responses of the ideal system and the two systems with coupling points at CP1 and CP2

III. Coupling Point Analysis

A. A Metric for Distortion

In this paper, distortion is a transfer function that is defined as the difference between the reference dynamics R_d and actual dynamics P, where R_d represents the dynamics of a HIL setup that is not distributed and P represents the dynamics of the same HIL setup distributed across the Internet. It is also useful to normalize distortion by the reference dynamics R_d, yielding the following:

$$\Theta = \frac{P - R_d}{R_d} \tag{1}$$

This definition of distortion was first introduced by Griffiths et al. within the haptics domain, where R_d represented the dynamics desired to be rendered to the user through the haptic device, and P represented the actual dynamics rendered to the user (Griffiths et al. 2008).

In the following, an ID-HIL system is treated involving only two sites, called local and remote. The reference dynamics R_d in this case are achieved through an ideal coupling (involving bilateral communications without delay) of the local and remote dynamics. Fig. 4 depicts the reference dynamics in block diagram form, where G and G_r refer to the local and remote dynamics, respectively, u_1 is the external input to the local system, y_1 is the output of interest in the local system, and u_2 and y_2 are the coupling variables between the local and remote systems. Generally, the variables u_2 and y_2 are power-conjugate variables modeling an energetic connection, such as force and velocity in the mechanical domain, but this need not be true in every ID-HIL system. The desired system equations are given as

$$\begin{bmatrix} y_1 \\ y_2 \end{bmatrix} = \begin{bmatrix} G_{11} & G_{12} \\ G_{21} & G_{22} \end{bmatrix} \begin{bmatrix} u_1 \\ u_2 \end{bmatrix}$$
$$u_2 = G_r y_2 \tag{2}$$

from which the desired dynamics, R_d, from u_1 to y_1 can be derived as

$$R_d = \frac{G_{11} + \left(G_{12}G_{21} - G_{11}G_{22}\right)G_r}{1 - G_{22}G_r} = \frac{G_{11} + A}{1 - G_{22}G_r} \tag{3}$$

where $A = \left(G_{12}G_{21} - G_{11}G_{22}\right)G_r$. Making the coupling point explicit enables an analysis of the effects of choosing different coupling points.

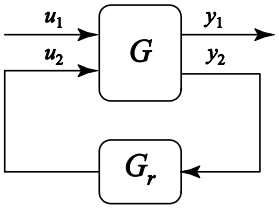

Fig. 4. Expressing the desired dynamics in block diagram form

Next, to capture the effect of delay due to the introduction of Internet communications in an ID-HIL setup, consider a multiplicative perturbation, Δ, to the remote dynamics, G_r. This multiplicative form is suitable for capturing the dynamics of Internet delay and could also capture other unmodeled dynamics such as the dynamics of the sensors and actuators. Fig. 5 expresses the adoption of the distortion metric into the ID-HIL framework in block diagram form, where distortion is the transfer function from u_1 to d.

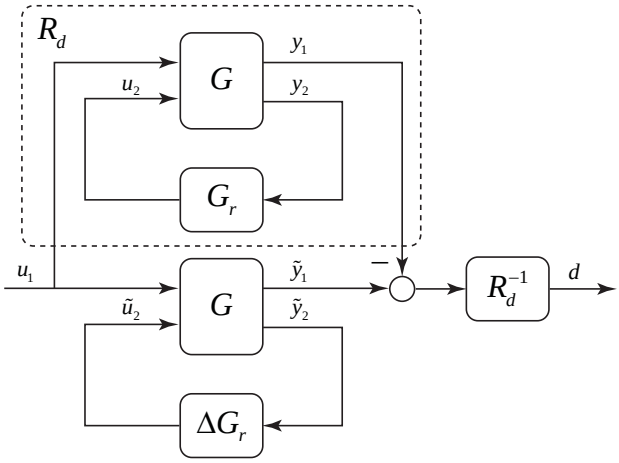

Fig. 5. Adoption of the distortion metric into the ID-HIL framework

The actual system equations become

$$\begin{bmatrix} \tilde{y}_1 \\ \tilde{y}_2 \end{bmatrix} = \begin{bmatrix} G_{11} & G_{12} \\ G_{21} & G_{22} \end{bmatrix} \begin{bmatrix} u_1 \\ \tilde{u}_2 \end{bmatrix}$$
$$\tilde{u}_2 = \Delta G_r \tilde{y}_2 \tag{4}$$

where tildes are used to differentiate the ideal variables from the actual variables. From Eq. (4), the actual dynamics P from u_1 to $\tilde{y}_1$ can be derived as

$$P = \frac{G_{11} + \Delta A}{1 - \Delta G_{22}G_r} \tag{5}$$

The distortion metric for the ID-HIL framework can then be found as

$$\Theta = \frac{P - R_d}{R_d} = \frac{G_{12}G_{21}G_r\left(\Delta - 1\right)}{\left(1 - \Delta G_{22}G_r\right)\left(G_{11} + A\right)} \tag{6}$$

Eq. (6) provides a means to analyze the impact on distortion of different coupling points in an ID-HIL system. Different coupling points will lead to different definitions of local and remote dynamics, i.e., different G_{11}, G_{12}, G_{21}, G_{22}, and G_r, even though the delay dynamics and other perturbation factors lumped in Δ may remain invariant, which is assumed to be the case in this paper. Therefore, different coupling points will, in general, yield different distortion values, and Eq. (6) can quantify their impact on distortion.

B. Distortion Analysis

In the framework created in section III.A, the ultimate goal of bringing the actual dynamics as close to the desired dynamics as possible translates to achieving a

distortion that is as small as possible. Since distortion is a transfer function and thus a function of frequency, it is also possible to define frequency ranges over which the distortion is desired to be small.

Eq. (6) reveals that there are a number of ways to achieve a small distortion at a given frequency. Specifically, besides the trivial case of $\Delta \equiv 1$, i.e., no perturbation, the distortion will be small for a given frequency, if one of the following is true at that frequency:

1. $G_{11} \to \infty$: the input u_1 is greatly amplified at the output y_1 and thus the contribution through the coupling with the remote system is negligible.
2. $G_{12} \to 0$: the feedback u_2 from the remote system has a very small effect on the output of interest y_1.
3. $G_{21} \to 0$: the external input u_1 has a very small effect on the coupling variable y_2.
4. $G_r \to 0$: the remote system does not affect the local system, i.e., it is driven by the local system without any impedance and the coupling is almost one-way.
5. $G_r \to \infty$: the remote system is acting almost like a wall, resisting even the smallest input y_2.
6. $G_{22} \to \infty$: the local impedance at the coupling point is so high that the local system is acting almost like a wall to the remote system.

Thus, to achieve low distortion, one should look for a coupling point that will lead to one of the conditions listed above. The physical interpretation associated with each condition can help making the assessments by inspection. However, it may not always be possible to observe that one of these conditions would be satisfied perfectly. In that case, it will be necessary to consider all the conditions simultaneously when comparing coupling points, which may make it difficult to utilize physical insight. Nevertheless, although the conditions above may seem unrelated at first sight, there actually exists a concept that unifies them all, and that concept is the sensitivity of the desired dynamics to the remote dynamics. A formal definition is given by

$$S_r \triangleq \frac{\partial R_d / R_d}{\partial G_r / G_r} \tag{7}$$

In words, it is defined as the ratio of a relative change in the desired dynamics to a relative change in the remote dynamics. Evaluation of S_r for the framework given in Fig. 4 leads to

$$S_r = \frac{G_{12}G_{21}G_r}{\left(1-G_{22}G_r\right)\left(G_{11}+A\right)} \tag{8}$$

Comparing Eq. (6) and (8), the following relationship between distortion and sensitivity to remote dynamics can be derived:

$$\Theta = S_r \frac{1-G_{22}G_r}{1-\Delta G_{22}G_r}\left(\Delta-1\right) \tag{9}$$

From Eq. (9) it can be seen that distortion will be small when the sensitivity to remote dynamics is small, and it can be easily verified that the conditions listed previously are also the conditions under which S_r becomes small. Hence, S_r provides a unifying concept for those conditions and also a single intuitive, physical explanation for distortion. Also, this sensitivity function may be more easily generalized to nonlinear systems than the distortion metric.

Furthermore, expanding the expression for distortion in Eq. (6) in a Taylor series around $\Delta = 1$ shows that, to a first order approximation, distortion is given by $S_r\left(\Delta-1\right)$, i.e.,

$$\Theta = S_r\left(\Delta-1\right) + O\left(\left(\Delta-1\right)^2\right) \tag{10}$$

Thus, to a first order approximation, and recalling that Δ is assumed to be invariant to the location of the coupling point, the difference in distortions caused by different coupling points is completely captured by the sensitivity function S_r. The significance of this finding can be seen by referring to Eq. (8) and noting that S_r can be evaluated without the knowledge of the perturbation Δ. Therefore, S_r not only provides a single metric to be considered when comparing coupling points, but also this metric is, unlike Θ itself, is independent of Δ. This allows for comparing coupling points without having to derive an expression for Δ.

Eq. (10) further implies that

$$S_r = \frac{\partial R_d / R_d}{\partial G_r / G_r} = \left.\frac{\partial \Theta}{\partial \Delta}\right|_{\Delta=1} \tag{11}$$

That is, the sensitivity S_r is the gradient of the distortion metric with respect to the perturbation Δ at $\Delta = 1$, i.e., the case when there is no perturbation.

Having related S_r to Θ, we can now go back to Eq. (7) to explain how a coupling point can be selected. Distortion will be small if a relative change in the remote dynamics creates a small relative change in the desired dynamics. Thus, the task of finding the best coupling point now translates to finding the coupling point that partitions into G_r all the dynamics whose relative change affects the desired system dynamics the least.

C. On the Signal Dependence of Distortion

It is important to note that distortion is defined for a particular output of interest y_1. Even though the formulation allows y_1 to be any signal in the local system, a low distortion in y_1 does not necessarily imply that the distortion will be low in *all* signals in the local system. This is easily demonstrated by considering the distortions in y_1 and y_2 simultaneously.

Following the same steps as for y_1, the distortion in y_2 can be derived as

$$\Theta_{y_2} = \frac{G_{22}G_r\left(\Delta-1\right)}{1-\Delta G_{22}G_r} \tag{12}$$

Thus, it can be seen that, besides the trivial condition $\Delta \to 1$ (i.e., no perturbation), there is only one condition under which both Θ and Θ_{y_2} become small, namely, $G_r \to 0$. The conditions 1, 2, 3, 5, and 6 do not necessarily imply a small Θ_{y_2}, and the condition $G_{22} \to 0$, which makes Θ_{y_2} small, does not necessarily make Θ small. This emphasizes the fact that distortion is not an independent property of the system, but is output-

signal dependent, as observed experimentally before (Ersal et al. in press b). Therefore, when considering a distortion analysis, it is important to keep the signals in mind with respect to which distortion was defined.

D. On the Effect of Causality on Distortion

Under some conditions, distortion can be improved simply by changing the causality. Consider the case when $G_{22} \to 0$. Furthermore, assume that G_{22}^{-1} and G_r^{-1} are proper. In this case, a switch in causality as shown in Fig. 6 leads to the following ideal system equations

$$\begin{bmatrix} y_1 \\ u_2 \end{bmatrix} = \begin{bmatrix} G_{11} & G_{12}G_{22}^{-1} \\ -G_{21}G_{22}^{-1} & G_{22}^{-1} \end{bmatrix} \begin{bmatrix} u_1 \\ y_2 \end{bmatrix} \qquad (13)$$
$$y_2 = G_r^{-1} u_2$$

which gives

$$R_d^* = \frac{G_{12}G_{21} + G_{11}G_{22}\left(1 - G_{22}G_r\right)}{G_{22}\left(1 - G_{22}G_r\right)} \qquad (14)$$

where the asterisk is used to denote the switched-causality case. Assuming a multiplicative perturbation Δ as before leads to

$$P^* = \frac{\Delta G_{12}G_{21} + G_{11}G_{22}\left(\Delta - G_{22}G_r\right)}{G_{22}\left(\Delta - G_{22}G_r\right)} \qquad (15)$$

Finally, the expression for distortion is obtained as

$$\begin{aligned} \Theta^* &= \frac{P^* - R_d^*}{R_d^*} \\ &= \frac{(1-\Delta)G_{12}G_{21}G_{22}G_r}{\left(\Delta - G_{22}G_r\right)\left(G_{12}G_{21} + G_{11}G_{22}\left(1 - G_{22}G_r\right)\right)} \end{aligned} \qquad (16)$$

From Eq. (16) it can be seen that

$$\lim_{G_{22} \to 0} \Theta^* = 0 \qquad (17)$$

Thus, distortion is reduced by switching the causality at the coupling point. Note that, in practice, such switching may require filters to ensure proper transfer functions.

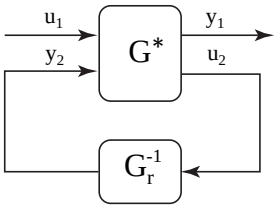

Fig. 6. Switching causality at the coupling point

IV. Application to the Example

In this section, the theory that is presented in Section III is applied to the quarter-car example introduced in Section II for illustration purposes.

An analysis of distortion using the proposed framework provides a frequency domain explanation into the different performances observed with the two coupling points for the same delay conditions. Fig. 7 compares the distortion metric for the two coupling points. As the figure clearly shows, the distortion for the system with CP2 is much less than the distortion for the system with CP1 at all frequencies, and hence, CP2 is a better choice of coupling point than CP1. The fact that the distortion is on the order of 1 around 50 rad/s for CP1 is the dominant reason for the significant difference between CP1 and ideal response in Fig. 3, whereas the close agreement between the ideal system and the system with CP2 is due to the fact that the magnitude of distortion is below -40 dB at all frequencies for CP2.

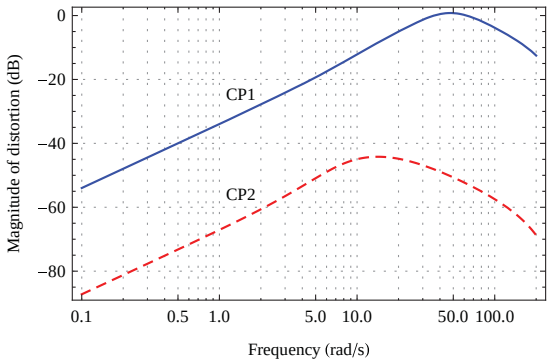

Fig. 7. The magnitude of the distortion metric for the two coupling points CP1 and CP2

To gain more physical insight, Fig. 8 compares the sensitivity, S_r, of the desired dynamics to the remote dynamics for the two coupling points CP1 and CP2. The sensitivity S_r is less for CP2 than CP1 for all frequencies, explaining why the distortion with CP2 is lower relative to the distortion with CP1.

Fig. 9 further reveals more in detail why the sensitivity S_r, and thus distortion, is low for CP2 by showing the magnitudes of the transfer functions G_{ij}, $i, j = 1, 2$, and G_r. Specifically, the distortion is low due to G_{12} that remains small across the entire frequency range. Physically, this corresponds to the fact that the driver and seat subsystem has a very small effect on the rest of the vehicle, because the reaction forces of the driver and seat subsystem have only a small effect on the sprung mass, which is the largest mass in the system. When this mass is considered as part of the remote system, as is the case with CP1, the sensitivity of the desired dynamics to the remote system increases, which explains the higher sensitivity and distortion observed for CP1.

Finally, Fig. 10 shows the magnitude plot of G_{22} for CP1. The magnitude being significantly greater than zero implies that distortion cannot be improved by reversing the causality at CP1. Thus, improving distortion for CP1 requires other methods such as feedback and/or feedforward control. Development of such methods, however, is beyond the scope of this paper.

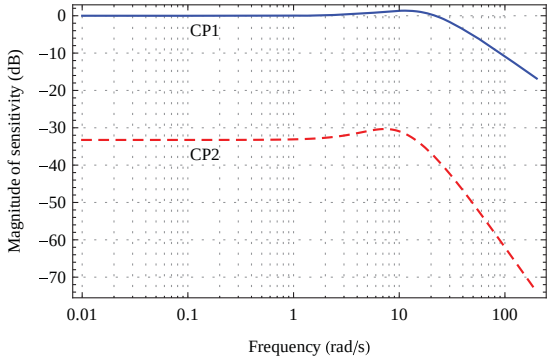

Fig. 8. The magnitude of sensitivity of the desired dynamics to the remote dynamics for the two coupling points CP1 and CP2

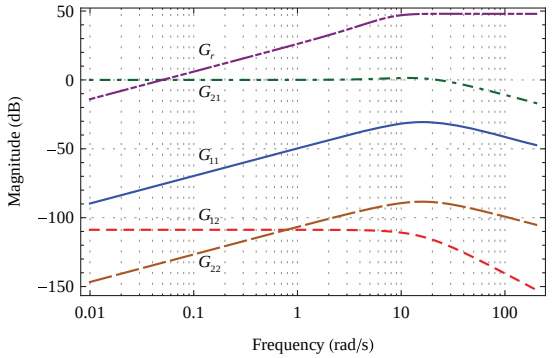

Fig. 9. The magnitude of G_{ij}, $i, j = 1, 2$, and G_r for CP2 as factors affecting sensitivity S_r

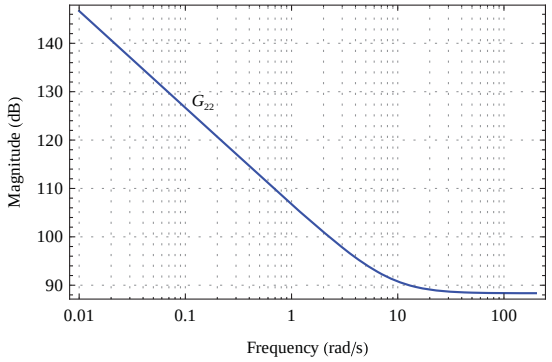

Fig. 10. The magnitude of G_{22} for CP1

V. Conclusion

The original contributions of this paper can be summarized as follows. This paper considers the coupling point as a design variable in ID-HILS systems and proposes a framework for a frequency-domain analysis of the impact of the coupling point location to distortion. A distortion metric from the haptics literature is adopted into this framework. Using this framework and metric, the paper identifies the system characteristics that render a coupling point location suitable for ID-HILS in the sense that it leads to a low distortion. The paper further identifies the sensitivity of the desired dynamics to the dynamics of the remote system as the unifying reason for different distortion results obtained with different coupling points. It also shows that distortion is an output-signal dependent concept and can, in some cases, be affected not only by the location of the coupling point, but also by the coupling causality. The paper applies this theory to a quarter-car model to illustrate and explain the differences between two coupling points.

Future work will focus on how distortion can be improved using feedback and how the choice of coupling point affects the trade-off between distortion attenuation and closed-loop sensitivity. Other potential future directions include extending these results to nonlinear systems, as well as considering the effects of distributed simulation, jitter, and loss, and the coupling of more than two subsystems.

References

Aghili, F. and J.-C. Piedboeuf (2002). Contact dynamics emulation for hardware-in-loop simulation of robots interacting with environment. 2002 IEEE International Conference on Robotics and Automation, IEEE.

Anderson, R. J. and M. W. Spong (1989). "Bilateral control of teleoperators with time delay." IEEE Transactions on Automatic Control **34**(5): 494-501.

Bacic, M., S. Neild and P. Gawthrop (2009). "Introduction to the special issue on hardware-in-the-loop simulation." Mechatronics **19**(7): 1041-1042.

Brudnak, M., M. Pozolo, V. Paul, S. Mohammad, W. Smith, M. Compere, J. Goodell, D. Holtz, T. Mortsfield and A. Shvartsman (2007). Soldier/Harware-in-the-loop simulation-based combat vehicle duty cycle measurement: Duty cycle experiment 2. Simulation Interoperability Workshop, Norfolk, VA, Simulation Interoperability Standards Organization (SISO).

Buford, J. A., Jr., A. C. Jolly, S. B. Mobley and W. J. Sholes (2000). Advancements in hardware-in-the-loop simulations at the U.S. Army Aviation and Missile Command. SPIE - Technologies for Synthetic Environments: Hardware-in-the-Loop Testing V, SPIE.

Cai, G., B. M. Chen, T. H. Lee and M. Dong (2009). "Design and implementation of a hardware-in-the-loop simulation system for small-scale UAV helicopters." Mechatronics **19**(7): 1057-1066.

Çavuşoğlu, M. C., A. Sherman and F. Tendick (2002). "Design of bilateral teleoperation controllers for haptic exploration and telemanipulation of soft environments." IEEE Transactions on Robotics and Automation **18**(4): 641-647.

Compere, M., J. Goodell, M. Simon, W. Smith and M. Brudnak (2006). "Robust control techniques enabling duty cycle experiments utilizing a 6-DOF crewstation motion base, a full scale combat hybrid electric power system, and long distance internet communications." SAE Technical Paper.

De Gersem, G., H. Van Brussel and F. Tendick (2005). "Reliable and enhanced stiffness perception in soft-tissue telemanipulation." International Journal of Robotics Research **24**(10): 805-822.

Elhajj, I., X. Ning, F. Wai Keung, L. Yun-Hui, Y. Hasegawa and T. Fukuda (2003). "Supermedia-enhanced Internet-based telerobotics." Proceedings of the IEEE **91**(3): 396-421.

Ersal, T., M. Brudnak, A. Salvi, J. L. Stein, Z. Filipi and H. K. Fathy (in press a). "Development and model-based transparency analysis of an Internet-distributed hardware-in-the-loop simulation platform." Mechatronics.

Ersal, T., M. Brudnak, J. L. Stein and H. K. Fathy (in press b). "Statistical transparency analysis in Internet-distributed hardware-in-the-loop simulation." IEEE/ASME Transactions on Mechatronics.

Ersal, T., B. Kittirungsi, H. K. Fathy and J. L. Stein (2009). "Model reduction in vehicle dynamics using importance analysis." Vehicle System Dynamics **47**(7): 851–865.

Fathy, H. K., Z. S. Filipi, J. Hagena and J. L. Stein (2006). Review of hardware-in-the-loop simulation and its prospects in the automotive area. SPIE - Modeling and Simulation for Military Applications, Kissimmee, FL, United States, SPIE.

Ganguli, A., A. Deraemaeker, M. Horodinca and A. Preumont (2005). "Active damping of chatter in machine tools - Demonstration with a

'hardware-in-the-loop' simulator." Journal of Systems and Control Engineering **219**(5): 359-369.

Goodell, J., M. Compere, M. Simon, W. Smith, R. Wright and M. Brudnak (2006). "Robust control techniques for state tracking in the presence of variable time delays." SAE Technical Paper.

Griffiths, P. G., R. B. Gillespie and J. S. Freudenberg (2008). "A fundamental trade off between performance and sensitivity within haptic rendering." IEEE Transactions on Robotics **24**(3): 537-548.

Huber Jr, E. G. and R. A. Courtney (1997). Hardware-in-the-loop simulation at Wright Laboratory's Dynamic Infrared Missile Evaluator (DIME) Facility. 1997 Technologies for Synthetic Environments: Hardware-in-the-Loop Testing II, SPIE.

Kelf, M. A. (2001). Hardware-in-the-loop simulation for undersea vehicle applications. SPIE - Technologies for Synthetic Environments: Hardware-in-the-Loop Testing VI, SPIE.

Kimura, A. and I. Maeda (1996). Development of engine control system using real time simulator. 1996 IEEE International Symposium on Computer-Aided Control System Design.

Lawrence, D. A. (1993). "Stability and transparency in bilateral teleoperation." IEEE Transactions on Robotics and Automation **9**(5): 624-637.

Lee, D. and M. W. Spong (2006). "Passive bilateral teleoperation with constant time delay." IEEE Transactions on Robotics **22**(2): 269-281.

Leitner, J. (2001). A hardware-in-the-loop testbed for spacecraft formation flying applications. 2001 IEEE Aerospace Conference, IEEE.

Mahin, S., R. Nigbor, C. Pancake, R. Reitherman and S. Wood (2003). The establishment of the NEES consortium. 2003 ASCE/SEI Structures Congress and Exposition: Engineering Smarter, American Society of Civil Engineers.

Mosqueda, G., B. Stojadinovic, J. Hanley, M. Sivaselvan and A. M. Reinhorn (2008). "Hybrid seismic response simulation on a geographically distributed bridge model." Journal of Structural Engineering **134**(4): 535-543.

Niemeyer, G. and J.-J. E. Slotine (1991). "Stable adaptive teleoperation." IEEE Journal of Oceanic Engineering **16**(1): 152-162.

Niemeyer, G. and J.-J. E. Slotine (2002). Toward bilateral Internet teleoperation. Beyond webcams: an introduction to online robots, MIT Press**:** 193-213.

Pan, P., M. Tada and M. Nakashima (2005). "Online hybrid test by internet linkage of distributed test-analysis domains." Earthquake Engineering and Structural Dynamics **34**(11): 1407-1425.

Spencer, B. F., A. Elnashai, N. Nakata, H. Saliem, G. Yang, J. Futrelle, W. Glick, D. Marcusiu, K. Ricker, T. Finholt, D. Horn, P. Hubbard, K. Keahey, L. Liming, N. Zaluzec, L. Pearlman and E. Stauffer (2004). The MOST Experiment: Earthquake Engineering on the Grid, NEESgrid.

Stojadinovic, B., G. Mosqueda and S. A. Mahin (2006). "Event-driven control system for geographically distributed hybrid simulation." Journal of Structural Engineering **132**(1): 68-77.

Tsai, K.-C., C.-C. Yeh, Y.-S. Yang, K.-J. Wang, S.-J. Wang and P.-C. Chen (2003). Seismic hazard mitigation: Internet-based hybrid testing framework and examples. International Colloquium on Natural Hazard Mitigation: Methods and Applications, France.

Verma, R., D. Del Vecchio and H. K. Fathy (2008). "Development of a scaled vehicle with longitudinal dynamics of an HMMWV for an ITS testbed." IEEE/ASME Transactions on Mechatronics **13**(1): 46-57.

Watanabe, E., T. Kitada, S. Kunitomo and K. Nagata (2001). Parallel pseudodynamic seismic loading test on elevated bridge system through the Internet. 8th East Asia-Pacific Conference on Structural Engineering and Construction, Singapore.

White, G. D., R. M. Bhatt, C. P. Tang and V. N. Krovi (2009). "Experimental evaluation of dynamic redundancy resolution in a nonholonomic wheeled mobile manipulator." IEEE/ASME Transactions on Mechatronics **14**(3): 349-357.

Xi, N. and T. J. Tarn (2000). "Stability analysis of non-time referenced Internet-based telerobotic systems." Robotics and Autonomous Systems **32**(2): 173-178.

Yokokohji, Y. and T. Yoshikawa (1994). "Bilateral control of master-slave manipulators for ideal kinesthetic coupling - formulation and experiment." IEEE Transactions on Robotics and Automation **10**(5): 605-619.

Yue, X., D. M. Vilathgamuwa and K.-J. Tseng (2005). "Robust adaptive control of a three-axis motion simulator with state observers." IEEE/ASME Transactions on Mechatronics **10**(4): 437-448.

Zhang, R. and A. G. Alleyne (2005). "Dynamic emulation using an indirect control input." Journal of Dynamic Systems, Measurement and Control **127**(1): 114-124.